

## UPGRADED CAVITIES FOR THE CEBAF CRYOMODULE REWORK PROGRAM\*

R. Rimmer<sup>†</sup>, G. Cheng, G. Ciovati, W. Clemens, E. Daly, K. Davis, J. Follkie, D. Forehand, F. Fors,  
J. Guo, J. Henry, K. Macha, F. Marhauser, L. Turlington, G. R. Myneni  
Thomas Jefferson National Accelerator Facility, Newport News, VA 23606 USA

### Abstract

The CEBAF cryomodule rework program has been a successful tool to recover and maintain the energy reach of the original baseline 6 GeV accelerator. The weakest original modules with eight five-cell cavities assembled in four “pairs”, with a specification when new of 20 MV per cryomodule (5 MV/m), are disassembled, re-cleaned with modern techniques and re-qualified to at least 50 MV (12.5 MV/m), (leading to the acronym “C50”). The cost per recovered MV is much less than building new modules. However over time the stock of weak modules is being used up and the voltage gain per rework cycle is diminishing. In an attempt to increase the gain per cycle it is proposed to rework the cavities by replacing the original accelerating cells with new ones of an improved shape and better material. The original CEBAF HOM and FPC end groups are retained. The goal is to achieve up to 75 MV (19 MV/m) for the reworked module (“C75”). Three C75 5-cell prototype cavities have been fabricated, processed and tested as part of an R&D program aiming at providing cavities to be installed during the refurbishment of some of the original CEBAF cryomodules. We report on the fabrication experience and test results of the first trial pair, containing two such reworked cavities.

### INTRODUCTION

In order to improve the energy gain of refurbished original CEBAF cryomodules with minimal cost, it was proposed to replace the cavity cells with newer ones of a new shape and material, which would allow achieving both higher accelerating gradient and quality factor than the original cavities. The end groups would be cut from existing cavities and welded to the new multi-cell structure to save as much of the existing cavity components as practically possible. The cell shape was chosen to be the ‘high current’ shape designed for a proposed high power FEL at JLab [1]. The material was chosen to be ingot Nb, a cavity material technology pioneered at Jefferson Lab since 2004 [2]. The performance specification is an accelerating gradient,  $E_{acc}$ , of 19 MV/m with a quality factor,  $Q_0$ , greater than  $8 \times 10^9$  at 2.07 K. Three prototype cavities were built and the two with the best RF performance were assembled into a cavity pair to be installed in the cryomodule currently being refurbished, which is planned to be installed in CEBAF in August 2017.

\* Authored by Jefferson Science Associates, LLC under U.S. DOE Contract No. DE-AC05-06OR23177. The U.S. Government retains a non-exclusive, paid-up, irrevocable, world-wide license to publish or reproduce this manuscript for U.S. Government purposes.

<sup>†</sup> rimmer@jlab.org

### CAVITY DESIGN

The cell shape adopted for the C75 cavity has the advantage of a ~14% lower  $E_p/E_{acc}$ , ~10% lower  $B_p/E_{acc}$  and ~10% higher R/Q·G compared to those of the Original Cornell (OC) shape, while having the same cell-to-cell coupling. Therefore the C75 cell shape has a more efficient design without compromising the HOM damping. The 5-cell cavity is designed to be field-flat by trimming each end half-cell by ~4 mm at the flat equator region, made from the same cup shape as used as for mid-cells. For the condition of maximum beam loading (460  $\mu$ A beam current) and for the peak detuning by microphonics of ~20 Hz [3], the minimum RF power to operate the C75 cavities would be achieved for a  $Q_{ext}$  of  $\sim 2.5 \times 10^7$ , compared to the  $Q_{ext} \sim 6.6 \times 10^6$  for the original CEBAF cavities. In order to achieve higher  $Q_{ext}$ -values, the distance between the end-cell and the fundamental power-coupler was increased by adding a Nb beam-tube ~40 mm long.

A draw-back of the C75 cell shape is that it has flat walls, which makes it less stiff compared to the OC shape. To mitigate this, stiffening rings are added between inner cells and between the end-cells and the end-groups. The position of the stiffening rings was determined by finite element analysis and verified experimentally [4] such that the C75 cavity would have the same stiffness as that of the OC CEBAF cavity, since the same cold tuner will be used.

### CAVITY MATERIAL

Two Nb ingots produced by CBMM, Brazil, as part of the company’s R&D program and sent to Jefferson Lab for evaluation and testing, were used for the fabrication of cavities 5C75-001 and 5C75-002. A center hole was cut by wire electro-discharge machining and the ingots were sliced into 3.175 mm thick discs with a multi-wire slicing machine at Slicing Tech, Inc. The thickness tolerance achieved was  $\pm 0.1$  mm and the average surface roughness was better than 1.6  $\mu$ m. Additional ingot Nb discs to build 5C75-003 were purchased from Tokyo-Denkai (TD), Japan. Table 1 summarizes the material and its properties for each cavity. The use of a material with lower residual resistivity ratio (RRR) can be advantageous to achieve a higher quality factor, which is very beneficial for CW accelerators [5]. Medium purity (RRR = 100-200) ingot Nb material is an ideal combination to achieve good performance at lower cost than standard fine-grain, high-purity (RRR > 250) Nb.

Table 1: Materials Used for the Fabrication of the Three Prototype Cavities

Cavity	Ingot SN	Supplier	RRR	Ta content (wt. ppm)
5C75-001	2370-5	CBMM	118	1350
5C75-002	2667-5	CBMM	114	670
5C75-003	NC-1654	TD	496	29

Several single-cell cavities were fabricated, processed and tested in order to check that the quality of the material allows achieving the required cavity performance. This was done as part of a broader R&D effort to evaluate the performance of ingot Nb cavities [5]. The results showed that buffered chemical polishing had a tendency to produce etch pits on the surface of medium and lower purity ingot Nb material and that centrifugal barrel polishing (CBP) followed by electropolishing (EP) were processing techniques better suited to achieve higher accelerating gradient with this type of material. On the other hand,  $E_{acc} > 30$  MV/m was easily achieved with high-purity ingot Nb cavities treated by BCP [6]. RF test results at 2.07 K showed that the material and processes adopted for the C75 cavities should allow achieving the  $Q_0$  and  $E_{acc}$  specifications with reasonable margin. Excellent performance both in terms of  $E_{acc}$  and Q-value was achieved in eleven 1.3 GHz, 9-cell cavities fabricated by industry from ingot Nb and tested at DESY [7].

## CAVITY FABRICATION

Niobium discs were pressed into half-cells with the standard deep-drawing method, using Aluminum dies and a 150 ton press. After deep-drawing and coining of the iris, the half-cells were subjected to a light chemical etch ( $\sim 10$   $\mu\text{m}$  removal) by BCP, followed by vacuum annealing at 800  $^\circ\text{C}/2$  h. The half-cells were then stamped and coined once more in order to mitigate spring-back effects and to achieve a shape closest to the design. A 3D color plot of the deviation of the shape of a half-cell from the shape of the die, shown in Fig. 1, indicates that the equator has a significant eccentricity. The maximum deviation from a round shape is  $\sim 0.4$  mm.

The extra material at both iris and equator of the half-cells after deep-drawing was cut by wire-EDM, leaving an additional length of 2.54 mm at both iris and equator for the final trimming. The iris of each half-cell was placed in a holding fixture, machined to a length 0.23 mm beyond the reference line and with 1.59 mm thick weld-preps by milling. The frequencies and Qs of the  $\text{TM}_{010-\pi}$  mode of each half-cell with a tube contacting the iris were measured with an RF testing fixture developed for C100 prototype cavities. Q-values above 3000 were typically achieved, which implies sufficiently good RF contact between a half cell and the RF fixture. The equator inner diameter and its roundness were measured with a CMM machine. The average frequency of all half-cells was 1.1 MHz lower than the target value. The average equator diameter was  $(176.4 \pm 0.1)$  mm, right on target, and the average roundness was 0.43 mm.

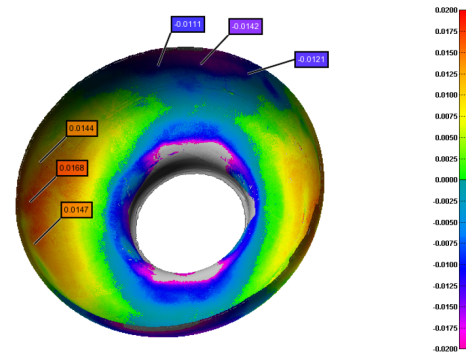


Figure 1: 3D plot of the point-to-point deviation of a C75 Nb half-cell from the die shape measured during an on-site demonstration of the ROMER 7525SI portable CMM scanner. Dimensions are in inches.

Dumb-bells were produced by electron-beam welding the irises from inside and outside, after  $\sim 20$   $\mu\text{m}$  etch of the iris region. Measurements of the length of half-cells and of corresponding dumb-bells consistently showed a weld-shrinkage of  $\sim 1$  mm, more than twice the expected value. The cause for this is unclear, however the additional length left at the iris was corrected for the set to be used for 5C75-003.

Niobium stiffening rings were machined and EB-welded to each dumb-bell. The equators on both sides of six dumbbells were trimmed by the same amount in a holding fixture by milling and subsequent measurements of the change in frequency and length were made in order to determine the trimming coefficient,  $df/dz = (-5.6 \pm 0.2)$  MHz/mm.

The material qualification study indicated that CBP and EP results in better performance than BCP for medium and low-purity ingot Nb cavities, however the CBP machine at JLab does not have large enough barrels to accommodate the fundamental power coupler (FPC) and higher-order modes (HOM) end-groups of a 5-cell cavity. Therefore it was decided to weld straight beam tubes to cavities 5C75-001 and 5C75-002, to allow for CBP.

End-groups from three spare cavities were cut by wire-EDM and two Nb adapter rings were machined to interface between the end-groups and the end-cells. End half-cells of 5C75-003 were welded to each end group. The dumb-bells' equators were trimmed to adjust the frequency and 1.59 mm thick weld-prep was machined by milling. The inner surface of the dumb-bells and end half-cells were lightly hand-polished with a grinding tool and aluminum oxide abrasive discs to remove any visible scratches and dints and to smoothen some of the grain boundary areas. The equator regions were etched to remove  $\sim 30$   $\mu\text{m}$ , followed by  $\sim 30$  min rinse with DI water with ultrasonic agitation. Two dumb-bells were sequentially EB welded to one end half-cell from the inside and outside and the same was done with two other dumb-bells, EB welded to the other end half-cell. The equator weld-preps were designed for a butt joint and the welds were done from the inside and outside. The final equator EB weld between two cavity halves was done from the outside. The end-groups were welded to 5C75-

Content from this work may be used under the terms of the CC BY 3.0 licence (© 2017). Any distribution of this work must maintain attribution to the author(s), title of the work, publisher, and DOI.

001 and 5C75-002 after cutting the straight beam tubes, after removing  $\sim 70 \mu\text{m}$  from the inner surface by centrifugal barrel polishing. Further details on the cavity fabrication can be found in [8]. A picture of 5C75-003 as fabricated is shown in Fig. 2.

The equator weld shrinkage was measured to be  $\sim 0.76 \text{ mm}$  per weld, rather than  $0.46 \text{ mm}$  initially estimated. This is due to the inside/outside EB welding. The larger than expected weld shrinkage was accounted for during machining of the dumb-bells for 5C75-001. The higher weld shrinkage resulted in higher frequencies for 5C75-002 and 5C75-003. The field flatness of the cavities after fabrication was  $>75\%$ . A blow-through hole in cell 4 (from the FPC side) during the outer equator weld had to be repaired in 5C75-001. Significant weld splatter occurred during outer welding of cell 4 in 5C75-002. Further investigation in the EB welding issues encountered during the cavities' fabrication showed the presence of faulty components in the EBW machine that needed to be replaced.



Figure 2: Picture of the fully welded 5C75-003 cavity.

## CAVITY PROCESSING AND TESTING

### 5C75-001 and 5C75-002

After fabrication the cavities were tuned to a field flatness  $>90\%$ . A list of the processing steps for each cavity leading to the first RF test is given in Table 2.

Table 2: List of Processing Steps of Cavities 5C75-001 and 5C75-002 after the End-groups were EB Welded

5C75-001	5C75-002
30 $\mu\text{m}$ EP	35 $\mu\text{m}$ EP
800 $^{\circ}\text{C}$ / 3 h vacuum anneal	800 $^{\circ}\text{C}$ / 3 h vacuum anneal
30 $\mu\text{m}$ EP	20 $\mu\text{m}$ EP
HPR	HPR

The average material removal was measured with an ultrasonic thickness probe at the same locations of each cavity cell. In preparation for the vertical tests, the cavities were assembled in an ISO 4 clean room. RF coupling was done using antennae protruding into each of the beam tubes. After slow pump-down on a test stand and leak check, oscillating superleak transducers (OSTs) were attached to the cavity cage to detect quench locations and flux-gate magnetometers were attached to the cavity to measure the residual magnetic field in the dewar during cooldown.

The RF test at 2.07 K of 5C75-001, shown in Fig. 4, was limited by a quench at 19.8 MV/m with a quality

factor of  $1.5 \times 10^{10}$ , without field emission. 5C75-002 quenched at 11 MV/m with a quality factor of  $9.6 \times 10^9$ , without field emission. In both cases, the residual field in the dewar was  $\sim 5 \text{ mG}$  during cool-down across  $T_c$ . The quench location was near the equatorial EB weld in cell 4 (from the FPC end group) for both cavities. An optical inspection of the cavities' inner surface near the quench location showed the presence of defects, shown in Fig. 3 for 5C75-001.

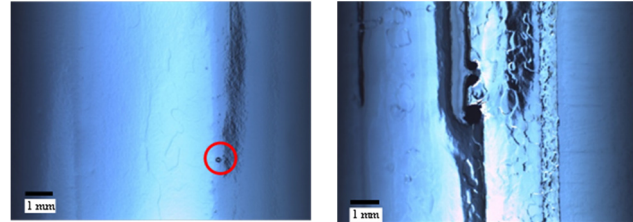


Figure 3: Defects found at the equator welds of cell 4 causing quenches in 5C75-001 (left) and 5C75-003 (right).

### 5C75-003

5C75-003 was tuned to  $>90\%$  field flatness, etched by BCP 1:1:2 removing  $\sim 95 \mu\text{m}$ , annealed in vacuum at  $600 \text{ }^{\circ}\text{C}$  for 10 h, electropolished to remove  $\sim 30 \mu\text{m}$ , degreased and high-pressure rinsed. The assembly, evacuation and cooldown procedures were the same as those of 5C75-001 and 5C75-002. For all C75 cavities, the cell temperature during EP was kept between  $18\text{--}22 \text{ }^{\circ}\text{C}$  and the cathode voltage at 13 V. The first RF test was limited by early field emission and RF cable breakdown at 9 MV/m. The cavity was disassembled, re-HPRed, assembled, evacuated, leak checked, and cooled-down in a  $\sim 3 \text{ mG}$  residual field. The second RF test was limited by quench at 15.6 MV/m with  $Q_0=7.8 \times 10^9$ , without field emission. The quench occurred at the equator EB weld of cell 4. Optical inspection of the inner cavity surface after warm-up and disassembly showed large ( $\sim 200 \mu\text{m}$  size) craters at the edge of the weld, as shown in Fig. 3. An attempt to repair the defects was made by local grinding using Cratex  $\text{Al}_2\text{O}_3$  abrasive cylinders in three steps, with coarse, medium and fine grit [9]. The defects were quite deep and it was not possible to completely remove them. After local grinding, the cavity inner surface was etched by BCP 1:1:2 removing  $\sim 30 \mu\text{m}$  followed by HPR, drying, assembly, evacuation. The results from the third RF test, shown in Fig. 4, indicated a quench at 15.9 MV/m with a  $Q_0$  of  $7.8 \times 10^9$  and some field emission. The quench was located in cell 5, near the equatorial EB weld. Optical inspection showed significant roughness of the weld area and a "surface relief"  $\sim 9 \text{ mm}$  away from the weld. Furthermore, severe pitting could be seen in cells 4 and 5, beyond  $\sim 2 \text{ cm}$  on both sides of the equator weld and some stains surrounding the pits, which could indicate insufficient rinsing of the cavity after BCP.

A summary of important parameters measured in preparation for and during the cryogenic RF tests is given in Table 3.

Table 3: Summary of RF Test Results of C75 Prototype Cavities

	5C75-001	5C75-002	5C75-003
$\Delta f$ (kHz) <sup>1</sup>	2783	2780	2788
$\Delta f/\Delta P$ (Hz/Torr)	-185	-178	-196
$E_{acc,max}$ (MV/m)	19.8	11	15.9
$Q_0(E_{acc,max}, 2.07\text{ K})$	$1.5 \times 10^{10}$	$9.6 \times 10^9$	$7.8 \times 10^9$
$R_{res}$ (n $\Omega$ )	$0.3 \pm 1$	$4.7 \pm 0.2$	$3.8 \pm 0.5$

<sup>1</sup>from 300 K, 1 atm to 2.07 K,  $10^{-7}$  mbar.

### 5C75-003 and 5C75-001 Cavity Pair

5C75-003 and 5C75-001 were prepared to be assembled into a cavity-pair for installation in cryomodule C50-7B (aka C50-13), following the same procedures as those for the preparation of C50 cavities. The only surface treatment done to the inner surface of 5C75-001 was degreasing and HPR, whereas 5C75-003 received an additional  $\sim 20\ \mu\text{m}$  EP to remove the acid stains observed after the last RF test, followed by degreasing and HPR.

For cavity pair testing, unlike for the vertical test as single cavities, a Nb “dog-leg”, a ceramic window and a Nb “top-hat” are assembled onto the FPC port of the cavity and Nb elbows with HOM loads are assembled to both HOM waveguide ports of each cavity. RF power is coupled into each cavity with an antenna in the top-hat and the field probe is located in a port on one of the HOM waveguides. The cavity pair was cooled down in a residual magnetic field of less than 5 mG. The results of the RF tests at 2.07 K are shown in Fig. 4. The results from the test of 5C75-001 show a decrease of  $Q_0$  by  $\sim 50\%$  compared to the results from the single-cavity test. Similar drop in  $Q_0$ -value was measured on an original CEBAF cavity after the dog-leg, ceramic window and top-hat were installed and seem to indicate additional RF losses from the brazed joint between the window and the stainless steel flange. This issue needs to be further investigated in order to achieve lower RF losses in the cryomodule.

Loaded Qs of HOMs have been measured at 4 K to check whether the most crucial dipole modes satisfy the beam break-up (BBU) impedance instability threshold for the CEBAF 12 GeV baseline machine operation ( $2.4 \times 10^{10}$  Ohm/m) [10]. Note that such HOM measurements are generally not carried out for refurbished C50 cavity pairs since the HOM-damping is known to be better than in C100 Low Loss (LL) upgrade cavities.

The impedance of each HOM was evaluated utilizing the product of the simulated R/Q-value and the measured Q-values ( $R/Q_{sim} \times Q_{meas}$ ). The corresponding results for the C75 cavity pair are shown in Fig. 5 comprising the most crucial TE<sub>111</sub> and TM<sub>110</sub> dipole passbands. Uncertainties remain concerning mode identification as not all existing HOMs could be detected with the used antennas probes. Modes below 1.9 GHz do not propagate into the HOM waveguides but are damped through the FPC. The assembly (dog-leg, ceramic window and top-

hat) attached to the cavity FPC port for the cavity pair test does not provide a sufficiently broadband absorbing condition as it is achieved in a cryomodule. Consequently, the Q-values of modes below 1.9 GHz are overestimated when measured in a cavity pair configuration. Overall, the results demonstrate that the impedance threshold for BBU (dashed line) is not exceeded even for the trapped TE<sub>111</sub> modes.

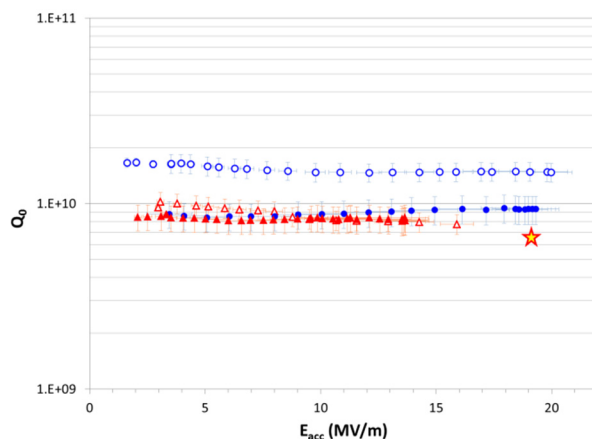


Figure 4:  $Q_0(E_{acc})$  at 2.07 K for 5C75-001 (circles) and 5C75-003 (triangles) measured as individual cavities (empty symbols) and assembled into a cavity pair with dog-leg, RF window and top-hat (solid symbols). The “star” symbol is the performance specification for the C75 cavities.

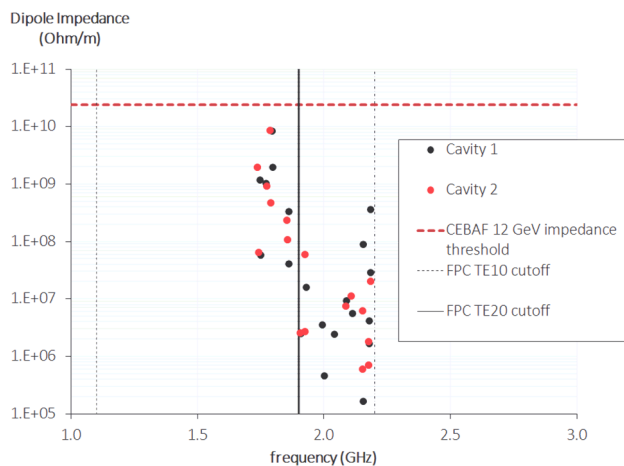


Figure 5: TE<sub>111</sub> and TM<sub>110</sub> dipole impedances for 5C75-001 and 5C75-003 assembled into a cavity pair.

## CRYOUNIT ASSEMBLY

Components with high remanent magnetic field have been identified as a cause of additional RF losses for the cavities inside original CEBAF cryomodules [11, 12]. In order to mitigate this issue, a new magnetic shield made of Cryoperm 10, 1 mm thick, was designed to fit closely to the cavities. A picture of 5C75-001 with the new magnetic shield and the cold tuners is shown in Fig. 6. Microphonics analysis and measurements were also done on C75 and C50 cavity pairs. As a result, aluminum/stainless steel brackets were added between the

HOM waveguides and the tuner yokes to raise the frequency of the mechanical modes associated with the motion of HOM waveguides.

Bracket for HOM waveguides      New magnetic shield

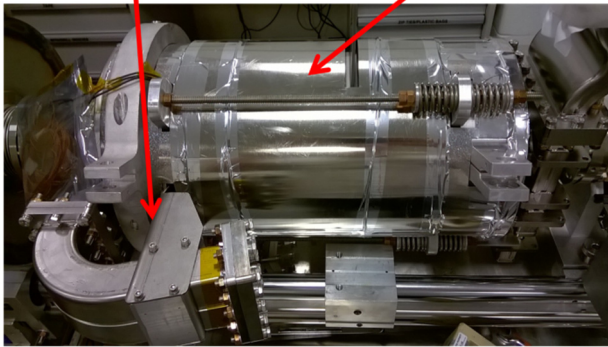


Figure 6: 5C75-001 with the new magnetic shield, cold tuner and bracket to fix the position of the HOM waveguide.

## CONCLUSION

Replacement of the cells of OC CEBAF cavities during the refurbishment of the least performing CEBAF cryomodules is a cost effective way to boost the energy gain of existing cryomodules. Three prototype ingot Nb cavities were built, processed and tested at JLab. The two best cavities, one made of Nb with RRR~120 and one made of RRR>300 Nb, are being installed in the next C50 cryomodule to be commissioned in CEBAF within 2017. The accelerating gradient was limited by defects in some of the equatorial welds. Faulty components found in the EBW machine are the leading cause for such defects. The HOM damping of the new cavity shape is adequate for operation of CEBAF at 12 GeV. A new magnetic shield was designed and installed on all cavities currently being assembled into the cryomodule to reduce residual RF losses due to trapped remanent field. Additional RF losses by the FPC window also need to be further understood and mitigated and additional thermal straps need to be added to the warm-to-cold transition FPC waveguide in order to reliably reduce the dynamic heat load.

Additional C75 cavities are expected to be built in the following months, either in house or by industry, to be installed in the next cryomodule refurbishment in 2018.

## ACKNOWLEDGMENTS

The medium purity Nb ingots were provided by CBMM as part of CRADA JSA 2004S002 between CBMM and Jefferson Lab.

## REFERENCES

- [1] H. Wang, R. Rimmer and G. Wu, "Elliptical Cavity Shape Optimization for Acceleration and HOM Damping", in *Proc. PAC'05*, Knoxville, TN, 2005, p. 4191.
- [2] P. Kneiel *et al.*, *Nucl. Inst. Meth. Phys. Res. A.*, vol. 774, pp. 133–150, 2015.
- [3] K. Davis and T. Powers, "Microphonics Evaluation for the CEBAF Energy Upgrade", JLab Tech Note TN-05-40, 2005.
- [4] G. Ciovati *et al.*, "Tuning sensitivity and stiffness of C20/C50 and C75 cavities", JLab Tech Note TN-17-017, 2017.
- [5] G. Ciovati, P. Dhakal and G. R. Myneni, *Supercond. Sci. Technol.*, vol. 29, p. 064002, 2016.
- [6] P. Kneisel, "Progress on large grain and single grain niobium - ingots and sheet and review of progress on large grain and single grain niobium cavities", in *Proc. SRF2007*, Beijing, China, 2007, p. 728.
- [7] W. Singer *et al.*, *Phys. Rev. ST Accel. Beams*, vol. 16, p.012003, 2013.
- [8] G. Ciovati *et al.*, "Experience with the fabrication, processing and testing of the prototype "C75" 5-cell cavities", Jefferson Lab Technical Note TN-17-029, 2017.
- [9] G. Massaro *et al.*, "Inspection and Repair Techniques for the EXFEL Superconducting 1.3 GHz Cavities at Ettore Zanon S.p.A: Methods and Results", *Proc. SRF'15*, Whistler, Canada, 2015, p. 368.
- [10] J. Guo and H. Wang, *Physics Procedia*, vol. 79, pp. 30-37, 2015.
- [11] R. L. Geng *et al.*, "Pursuing the origin and remediation of low  $Q_0$  observed in the original CEBAF cryomodules", in *Proc. IPAC'14*, Dresden, Germany, 2014, p. 2828.
- [12] G. Ciovati *et al.*, *IEEE Trans. Appl. Supercond.*, vol. 27, no. 4, p. 3500106, 2017.